

THE MAGNETIC SPECTROMETER PRISMA AT LNL

E. FIORETTO, L. CORRADI, A.M. STEFANINI, S. SZILNER*, B.R. BEHERA,
G. DE ANGELIS, A. GADEA, A. LATINA, G. MARON,
D.R. NAPOLI, A. PISENT, Y.W. WU

*INFN - Laboratori Nazionali di Legnaro, Viale dell'Università, 2
Legnaro (PD), 35020, Italy*

S. BEGHINI, G. MONTAGNOLI, F. SCARLASSARA

*Dipartimento di Fisica dell'Università and INFN Sezione di Padova, Via Marzolo 4
Padova, 35131, Italy*

M. TROTTA, A. DE ROSA, G. INGLIMA, M. LA COMMARA,
D. PIERROUSAKOU, M. ROMOLI, M. SANDOLI

*Dipartimento di Fisica dell'Università and INFN Sezione di Napoli, Via Cintia
Napoli, 80126, Italy*

G. POLLAROLO

*Dipartimento di Fisica dell'Università and INFN Sezione di Torino, Via P. Giuria 1
Torino, 10125, Italy*

The new magnetic spectrometer PRISMA for heavy-ions has been installed at the end of 2002 and is now operating at LNL. In-beam tests evidenced experimental resolutions consistent with the design characteristics of the setup. A first experimental campaign has been completed at the end of 2004.

1. Introduction

The magnetic spectrometer PRISMA [1,2,3] has been recently installed at LNL. It has been designed to be used with heavy-ion beams accelerated at energies up to $E = 5\text{-}10$ AMeV by means of the Tandem-ALPI accelerator complex of the Laboratori Nazionali di Legnaro. The next operation of the new superconductive injector PIAVE and its coupling with the ALPI Linac will allow to extend the nuclear physics studies in the $A=100\text{-}200$ mass region. Moreover, PRISMA is

* Present address: R. Boskovic Institute, Bijenicka c. 54, HR-10001 Zagreb, Croatia.

the natural candidate for use in future experiments with radioactive ion beams which will be produced by the proposed SPES facility at LNL.

The spectrometer is located in the East target area of the Tandem building and its commissioning has been completed at the beginning of 2003. In July of 2003 the installation of the γ -array CLARA [4] around the target point of PRISMA (in the backward hemisphere) was started. Such array is composed of 25 CLOVER detectors of the EUROBALL setup. The first experimental campaign started in April 2004.

Few- and multi-nucleon transfer reactions [5,6] (from grazing to deep-inelastic collisions), elastic and inelastic scattering will be studied with specific experiments by using PRISMA in order to extract the properties of the nuclear residual interaction and to understand the evolution of the single-particle levels. Moreover, binary reactions will be used as a powerful tool to populate moderately neutron-rich isotopes and to study the nuclear structure in interesting mass regions (near to ^{78}Ni and ^{132}Sn). These experiments will be performed in conjunction with the CLARA setup. The operation of the spectrometer in Gas-Filled Mode will allow to extend the nuclear dynamics studies to the fusion-evaporation reactions.

A detailed description of the spectrometer and its entrance and focal plane detectors will be given. The results of the in-beam tests and first experiments will be also reported.

2. The PRISMA setup

2.1. Spectrometer

The optical design of the spectrometer consists of a magnetic quadrupole (30 cm diameter, 50 cm long) followed at 60 cm by a 60° bending angle magnetic dipole (20 cm gap, 100 cm usable width, 120 cm curvature radius). A picture of the spectrometer is shown in Fig. 1. It is mounted on a rotating platform that allows rotations around the target point in the $-20^\circ \leq \theta \leq +130^\circ$ angular range with respect to the beam direction (an important requirement for the study of two-body reactions such as multi-nucleon transfer). A small sliding seal scattering chamber houses a couple of small area Si detectors ($\sim 50 \text{ mm}^2$) working as beam monitors and/or as normalization devices. The spectrometer is equipped with entrance and focal plane detectors that allow the complete identification and trajectory reconstruction of the reaction products by using the Time of Flight (TOF) and ΔE -E techniques together with the position information at the entrance and the focal plane, respectively.

The most interesting features of the spectrometer are:

- a solid angle of 80 msr;
- angular acceptances of $\Delta\theta = \pm 6^\circ$ and $\Delta\phi = \pm 11^\circ$;
- a momentum acceptance of $\pm 10\%$;
- a maximum rigidity around 70 AMeV;
- a mass resolution up to 1/300 (via TOF);
- an energy resolution up to 1/1000 (via TOF).

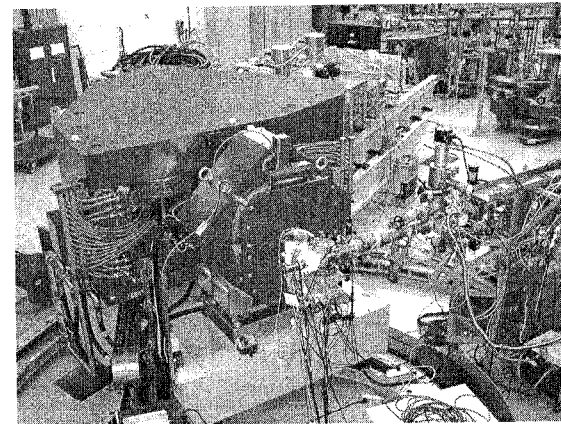


Figure 1. The PRISMA spectrometer placed at 90° with respect to the beam direction. The magnets are clearly seen on the rotating platform.

These performances are made possible by the software reconstruction of the ion tracks.

2.2. Entrance Detector

The entrance detector is composed of a double layer of large-area ($80 \times 100 \text{ mm}^2$) Micro-Channel Plates (MCP) mounted in the Chevron configuration [7]. Its high counting rate capability allowed to mount the detector close to the target (about 25 cm from it) where, usually, a very high background due to δ -electrons, X-rays and light charged particles is present. In this location it matches the whole solid angle covered by the spectrometer. The ejectiles coming from the target enter the active volume of the detector through a grid made of $20 \mu\text{m}$ gold-plated tungsten wires biased at the same high voltage of the MCP pair (typically around -2200 V). Then the ions impinge and pass through a thin self-supporting carbon foil ($\sim 20 \mu\text{g}/\text{cm}^2$), tilted by 45° with respect to the central trajectory and biased at about -2500 V, and enter into the PRISMA spectrometer. The backwards emitted

electrons are accelerated towards the MCP by means of the electric field produced by a second grid placed 4 mm apart from the carbon foil and biased at about -2200 V. In order to preserve the ion position information, a magnetic field of about 100-120 Gauss, parallel to the accelerating electric field, is applied using an external coil. The accelerated and focused electrons reach the MCP pair surface and undergo multiplication. The produced charge is collected by a position sensitive anode. It is composed of two orthogonal delay lines made of 70 μm Cu-Be wires wrapped around rounded plexiglass frames of two different diameters. The outer delay line is 3 mm apart from the MCP output face. The whole anode structure is directly fixed to the printed circuit board housing the home-made electronics for the signal processing. All electronics is installed in vacuum.

A picture of the detector is shown in Fig. 2.

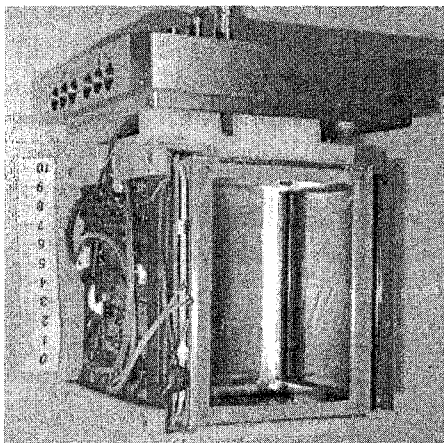


Figure 2. View of the MCP detector. The printed circuit board with the home-made electronics and the carbon foil are clearly visible on the left and on the right, respectively.

The detector provides a timing signal to be used as start reference for TOF measurements and for measuring the (X,Y) entrance position of the reaction products in the spectrometer. The position information is obtained from the difference in arrival time of the signal at one end of the delay line with respect to the reference time signal. The latter is extracted from the output face of MCP through a 100-240 pF capacitor.

2.3. Focal Plane Detector

The focal plane detector is composed of a large area Multi-Wire Parallel Plate Avalanche Counter (MWPPAC) followed by a transverse field multi-anode Ionization Chamber (IC) at about 50 cm of distance [8].

In order to match the large acceptance of the spectrometer, the MWPPAC covers a total active area of $100 \times 13 \text{ cm}^2$ and has a three electrode structure: a central cathode and two anodic wire planes (X and Y) orthogonally oriented to each other and symmetrically placed with respect to the cathode at a distance of 2.4 mm from it. The cathode is made of 20 μm diameter gold-plated tungsten wires with a spacing of 0.3 mm (3300 wires) and electrically divided in ten equal and independent sections. Each of them has an active area of $10 \times 13 \text{ cm}^2$ and provides a timing signal for both TOF measurements and Data Acquisition trigger. The X-plane is equally segmented as the cathode and each section consists of 100 wires of the same type with a spacing of 1 mm. The cathode and X-plane wires are soldered to a printed-circuit on G-10 frames. The Y-plane is common to all cathode sections with 130 wires (100 cm long, with the same diameter and 1 mm step as for the X wires) soldered on the other side of the same frame of the cathode. The cathode-anode gap is 2.4 mm. The position information is extracted from the X and Y anodes by using a delay-line readout. The cathode is biased at a negative high voltage (500-600 V with isobutane at working pressures of about 7-8 mbar) while the anodes are electrically grounded through 100 k Ω resistors. The detector is inserted in a stainless steel vessel closed on both sides by two large mylar windows ($100 \times 13 \text{ cm}^2$) facing the anodes wire planes at a distance of 3 mm. Windows are made of 1.5 μm thick mylar foils glued on a proper metallic frame and supported by 100 μm stainless steel wires spaced 3.5 mm. A picture of the MWPPAC is shown in Fig. 3.

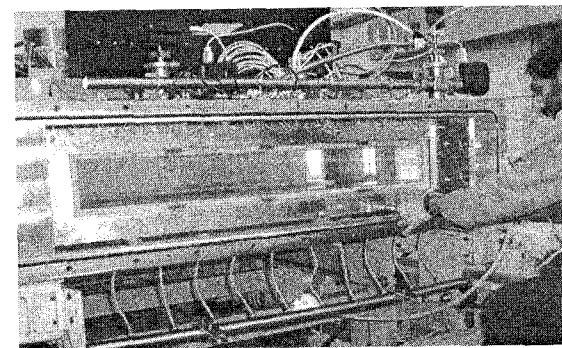


Figure 3. View of the MWPPAC inserted in its vacuum vessel.

The IC dimensions in the dispersion plane are $110 \times 17.6 \text{ cm}^2$ while the active depth is 120 cm. Its cathode and anode are divided in ten sections along the focal plane. Each of them is segmented in four pads (265.0 mm long by 99.0 mm wide) providing independent ΔE signals. This choice is an optimum compromise for preserving good Z and E resolution over the whole focal plane, where the event rate may overcome several kHz/section, keeping at a reasonable level the number of pads and consequently the electronic equipment. The cathode and anode are obtained by a photoengraving process of Cu layer deposited onto a 2 mm thick G-10 plate. The Frisch grid (common to all sections) is made of 1000 golden tungsten wires with a $100 \mu\text{m}$ diameter spaced 1 mm apart and 1 m long. The wires are soldered on both sides of a G-10 frame after proper stretching (100 g). The anode-Frisch grid and cathode-Frisch grid distances are 1.6 and 16 cm, respectively. The $1.5 \mu\text{m}$ thick mylar window is glued on a stainless steel nose and is supported by 1000 stainless steel wires ($100 \mu\text{m}$ thick, 1 mm step). The cathode (all pads) is held at ground potential while the Frisch grid and the anode are biased in such a way as to maximize the electron drift velocity in the active region and to minimize the shielding inefficiency of the Frisch grid in the collection region. The detector is routinely used with methane (CH_4 , 99% purity), mainly due to its high electron drift velocity. However for energetic heavy-ions, CF_4 has to be used because of its high stopping power and electron drift velocity.

3. In-beam tests and first experiments

The performances of the PRISMA spectrometer have been tested with several heavy-ion beams (^{32}S , ^{40}Ca , ^{56}Fe , ^{58}Ni , ^{82}Se , ^{90}Zr) at energies ranging from 4 to 6 AMeV impinging onto different targets.

A typical X (Y) position resolution of 1 mm (2 mm) has been obtained for the MWPPAC. Position spectra obtained for the 230 MeV $^{40}\text{Ca} + ^{208}\text{Pb}$ reaction are shown in Fig. 4. The different shapes of X and Y spectra are due to the PRISMA optics, i.e. dispersing in X and focusing in Y. The detector efficiency is close to 100% for a wide range of heavy-ions and energies when compared with the reference number of events collected in the IC placed downstream.

In Fig. 5 the ΔE -E scatter plot obtained with the IC for the 505 MeV $^{82}\text{Se} + ^{238}\text{U}$ reaction is shown for one of the central sections. Its multi-anode structure allows to optimize the partition between the ΔE and residual E in order to identify at the same time reaction products coming from very different nuclear processes. In fact, for this reaction the magnetic fields of the spectrometer select both transfer and fission-like fragments. A good identification of the different proton stripping (up to 8-10 proton transfer) and pick-up channels has been

evidenced. The fission fragments are well identified and separated from the transfer products because of their lower range in the IC.

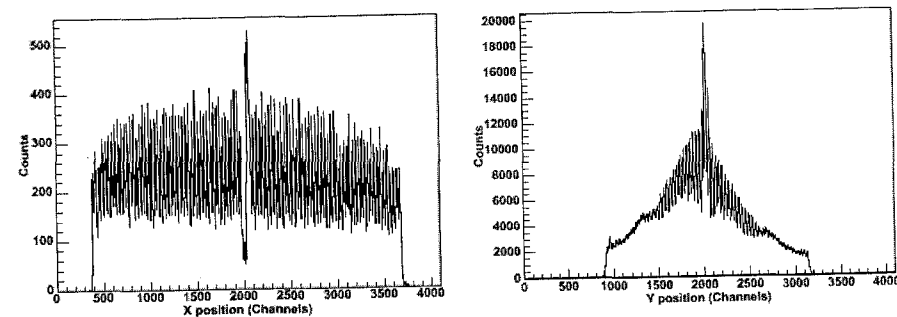


Figure 4. X (only one section) and Y position spectra obtained for the 230 MeV $^{40}\text{Ca} + ^{208}\text{Pb}$ reaction.

The Z resolving power is $Z/\Delta Z \sim 60$ evaluated for $Z=34$. The measured energy resolution is about 2%.

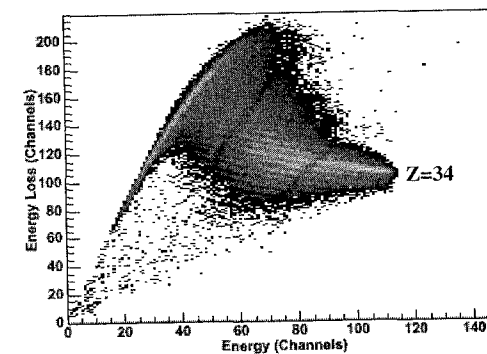


Figure 5. ΔE -E matrix obtained for the central section of the IC in the 505 MeV $^{82}\text{Se} + ^{238}\text{U}$ reaction.

The 235 MeV $^{40}\text{Ca} + ^{208}\text{Pb}$ ($50 \mu\text{g}/\text{cm}^2$) reaction was used to check the energy (momentum) resolution of PRISMA. Elastically and inelastically scattered ^{40}Ca ions were analyzed by means of PRISMA (placed at 90°) and identified at the focal plane. Fig. 6 shows the X position spectrum at the focal plane obtained by gating on $A=40$ in the mass spectrum and selecting events corresponding to $Z=20$ in the ΔE -E matrix of the IC with the condition $\Delta\theta \sim 1.5^\circ$ (gate on the position spectrum of the MCP). The elastic peak is clearly separated from the inelastic octupole excitations of both projectile and target. The deduced energy resolution is roughly 700 keV, corresponding to about 1/300, mainly depending on the target thickness and the reaction kinematics.

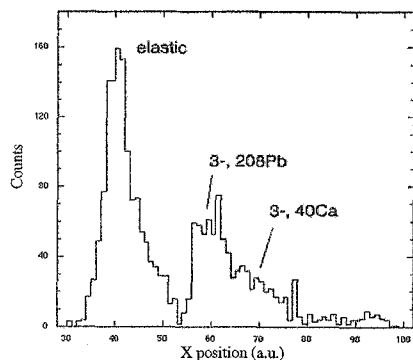


Figure 6. X position spectrum along the focal plane of PRISMA.

A significant test of the mass resolution was performed by studying the 263 MeV $^{58}\text{Ni} + ^{124}\text{Sn}$ reaction. The ejectiles were analyzed by PRISMA placed at $\theta_{\text{lab}} = 68^\circ$ (near the grazing angle) and several mass spectra have been obtained by selecting different Z in the ΔE - E matrix of the IC. Multi-proton stripping channels were mainly observed besides strong neutron pickups as expected from the Q -value systematics for the various reaction channels.

A typical X-TOF scatter plot obtained for one of the central section of the MWPPAC gated by a $10 \times 40 \text{ mm}^2$ window in the X-Y position matrix of the MCP is shown in Fig. 7.

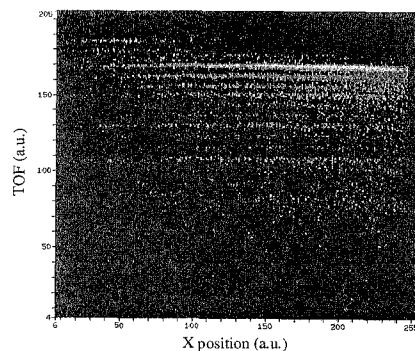


Figure 7. X-TOF scatter plot obtained for the 263 MeV $^{58}\text{Ni} + ^{124}\text{Sn}$ reaction.

The different bands correspond to different mass number (A) to atomic charge state (q) ratios for the reaction products analyzed by PRISMA. A mass resolution up to $\Delta A/A = 1/280$ was measured. This is also routinely obtained during the

experiments presently being performed using the PRISMA-CLARA combined facility.

An example of mass spectrum is reported in Fig. 8. It has been obtained in the 505 MeV $^{90}\text{Zr} + ^{208}\text{Pb}$ reaction after ion-track reconstruction and corresponds to the mass distribution of Zirconium isotopes for a part of the total accumulated statistics.

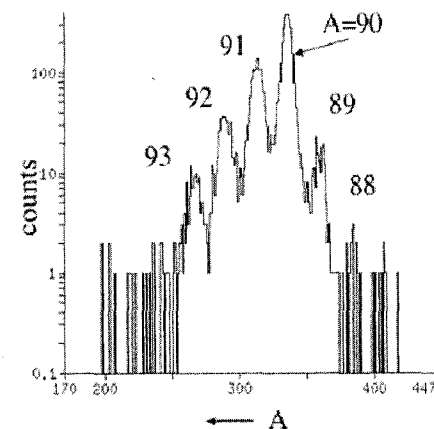


Figure 8. Zirconium isotopes populated by neutron transfer in the 505 MeV ^{90}Zr on ^{208}Pb .

The scattered Zr-like ions were analyzed by the magnetic spectrometer centered around the grazing angle ($\theta_{\text{lab}} \sim 62^\circ$). One sees that one- and multi-neutron pickup channels are favoured with respect to the stripping ones, as expected from Q -value systematics.

The first experimental campaign was started in April 2004. Up to now nine experiments have been performed with the PRISMA-CLARA setup. Many of these experiments have been devoted to nuclear structure studies and some of their main goals were:

- studying the shell closure in neutron-rich nuclei at $N=20$ and $N=28$;
- studying the shell closure evolution at the magic number $N=50$;
- the spectroscopy of neutron-rich nuclei in the $A=60$ mass region;
- studying the shell model in the ^{48}Ca region;
- studying the multi-nucleon transfer channels for the $^{90}\text{Zr} + ^{208}\text{Pb}$ reaction.

The data analysis of the experiments is in progress.

4. Next developments

The use of PRISMA in a “gas filled mode” (GFM) constitutes an important extension of its capabilities to the measurements of evaporation residues recoiling at or near to 0°. The GFM is characterized by high transmission efficiency (a very important feature in the case of low production cross sections) but the main drawback is the loss of mass and energy resolution. Then, PRISMA in GFM will be used as a separator rather than a spectrometer. In this configuration evaporation residues can be efficiently focused onto a reasonably small area at the exit of the magnetic dipole, where they can be implanted for decay studies (recoil- α tagging, α -decay studies, etc.).

Simulations for GFM operation of the PRISMA spectrometer are in progress. The first results seem to indicate that a suitable detection system for implanting the recoil nuclei could be composed of a matrix of 2x5 Si detectors with a thickness of 300 μm and an active area of 5x5 cm^2 . To get the position information Si strips will be used. A first prototype of this detection system is being assembled. The drift region existing downstream of the magnetic dipole was introduced mainly in order to increase the base for time of flight and ultimately to optimize the mass resolution in vacuum, but it is mostly useless in gas. Indeed the implantation system can be placed at only 60 cm of distance from the exit of the magnetic dipole.

5. Summary

The commissioning of the PRISMA+CLARA setup has been completed at the end of 2003. The in-beam tests and first experiments confirmed the performances foreseen for PRISMA and its detectors. Nine experiments have been already completed during 2004. The construction of the new detection system for the GFM operation of the PRISMA spectrometer is in progress.

References

1. A.M. Stefanini et al., *Nucl. Phys.* **A701**, 217c (2002).
2. F. Scarlassara et al., *Nucl. Phys.* **A746**, 195c (2004).
3. A. Latina et al., *Nucl. Phys.* **A734**, E1 (2004).
4. A.Gadea et al., *Eur. Phys. J.* **A20**, 193 (2004).
5. L. Corradi et al., *Phys. Rev.* **C66**, 024606 (2002).
6. S. Szilner et al., *Eur. Phys. J.* **A21**, 87 (2004).
7. G. Montagnoli et al., *INFN-LNL(REP)* - **202/2004**, 149 (2004).
8. E. Fioretto et al., *INFN-LNL(REP)* - **198/2003**, 148 (2003).

DESCRIPTION AND FIRST RESULTS OF THE CLARA-PRISMA SETUP

A.GADEA*, N.MARGINEAN, G.DE ANGELIS, D.R.NAPOLI, L.CORRADI,
E.FIORETTO, A.M.STEFANINI, J.J. VALIENTE-DOBÓN, S.SZILNER,
L.BERTI, P.COCCONI, D.ROSSO, N.TONIOLO, M.AXIOTIS, B.R.BEHERA,
A.LATINA, I.V.POKROVSKIY, C.RUSU, W.ZHIMIN
INFN, Laboratori Nazionali di Legnaro Padova, Italy

E.FARNEA, S.M.LENZI, C.A.UR, R.ISOCRATE, D.BAZZACCO, S.BEGHINI,
S.LUNARDI, G.MONTAGNOLI, R.MENEGAZZO, F.SCARLASSARA,
F.DELLA VEDOVA, M.NESPOLO, R.MARGINEAN,
Dipartimento di Fisica, Università and INFN Sez. di Padova, Italy

A.BRACCO, F.CAMERA, S.LEONI, B.MILLION, M.PIGNANELLI,
G.BENZONI, O.WIELAND
Dipartimento di Fisica Università and INFN Sez. di Milano, Italy

P.G.BIZZETI, A.M.BIZZETI-SONA
Dipartimento di Fisica, Università and INFN Sez. di Firenze, Italy

G.POLLAROLO
Dipartimento di Fisica, Università and INFN Sez. di Torino, Italy

M.TROTTA
Dipartimento di Fisica, Università and INFN Sez. di Napoli, Italy

AND THE CLARA AND PRISMA2 COLLABORATIONS.

*corresponding author (andres.gadea@lnl.infn.it)